

Chapter 2

The Mechanical Equilibrium of Rotating Stars

“Epur si muove” said Galileo Galilei when claiming that the Earth is rotating. Due to rotation, the equatorial radius of the Earth is about 21.4 km longer than its polar radius, so that the Mississippi from its source to the Gulf of Mexico is “raising” away from the Earth center. Of course, in terms of the equipotentials it is “descending” to the sea.

The same can also be said about the stars, where the effects of rotation are on the average much larger than on the Earth. In stars, the equatorial radius can be much bigger than the polar radius, up to about 1.5 times the polar radius. This shows the importance of the possible rotational effects. In addition, while the Earth rotates like a solid body, stars may have an internal differential rotation, with for example a core rotating faster than the outer envelope. Moreover, stellar rotation not only produces a flattening of the equilibrium configuration, but it drives internal circulation motions and various instabilities which transport both the chemical elements and the angular momentum.

2.1 Equilibrium Configurations

2.1.1 From Maclaurin Spheroids to the Roche Models

The stability of rotating configurations has been studied since long (see review in [315]), for example with Maclaurin spheroids, where the density ϱ is supposed constant or with the Roche model, which assumes an infinite central condensation. The complex reality lies between these two extreme cases.

In the case of the Maclaurin spheroids, the equilibrium configurations flatten for high rotation. For extremely high angular momentum, it tends toward an infinitely thin circular disk. The maximum value of the angular velocity Ω (supposed to be constant in the body) is $\Omega_{\max}^2 = 0.4494 \pi G \varrho$. In reality, some instabilities would occur before this limit is reached.

In the case of the Roche model with constant Ω (this is not a necessary assumption), the equilibrium figure also flattens to reach a ratio of 2/3 between the polar

and the equatorial radii, with a maximum angular velocity $\Omega_{\max}^2 = 0.7215 \pi G \bar{\rho}$, where $\bar{\rho}$ is the mean density (see Sect. 4.4.2). Interestingly enough, for all stellar masses the rotational energy of the Roche model amounts to at most about 1% of the absolute value of the potential energy of the models considered with their real density distributions. Except for the academic case of stars with constant density or nearly constant density, the Roche approximation better corresponds to the stellar reality. Recent results from long-baseline interferometry [94, 465] support the application of the Roche model in the cases of Altair and Achernar, which both rotate very fast close to their break-up velocities (see Sect. 4.2.3). These new possibilities of observations open interesting perspectives.

Here, we consider models of real stars, with no a priori given density distributions and obeying a general equation of state. The properties of rotating stars depend on the distribution $\Omega(r)$ in the stellar interiors. The first models were applied to solid body rotation, i.e., $\Omega = \text{const.}$ throughout the stellar interior. More elaborate models consider differential rotation, in particular the case of the so-called shellular rotation [632], i.e., with a rotation law $\Omega(r)$ constant on isobaric shells and depending on the first order of the distance to the stellar center (see Sect. 2.2). The reason for such a rotation law rests on the strong horizontal turbulence in differentially rotating stars, which imposes a constancy of Ω on isobars [632]. In the vertical direction, the turbulence is weak due to the stable density stratification.

Interestingly enough, recent models with rotation and magnetic fields give rotation laws $\Omega(r)$ rather close to solid body rotation (Sect. 13.6), nevertheless with some significant deviations from constant Ω . Thus, whether or not magnetic fields play a role, it is necessary to account for rotation laws which are not constant in stellar interiors during evolution.

2.1.2 Hydrostatic Equilibrium for Solid Body Rotation

We first consider the angular velocity $\Omega = \text{const.}$ throughout the star. Let us assume hydrostatic equilibrium and ignore viscous terms. The Navier–Stokes equation (1.2) becomes with account of the centrifugal acceleration

$$\frac{1}{\rho} \nabla P = -\nabla \Phi + \frac{1}{2} \Omega^2 \nabla (r \sin \vartheta)^2, \quad (2.1)$$

according to (B.24) and following remarks. $\varpi = r \sin \vartheta$ is the distance to the rotation axis (Fig. 2.1). The above expression of the centrifugal force gives a projection $\Omega^2 \varpi \sin \vartheta$ along vector \mathbf{r} and a projection $\Omega^2 \varpi \cos \vartheta$ along vector $\boldsymbol{\vartheta}$. The quantity Φ is the gravitational potential, which is unmodified by rotation in the Roche approximation,

$$\mathbf{g} = -\nabla \Phi = -\frac{GM_r}{r^2} \frac{\mathbf{r}}{r}. \quad (2.2)$$

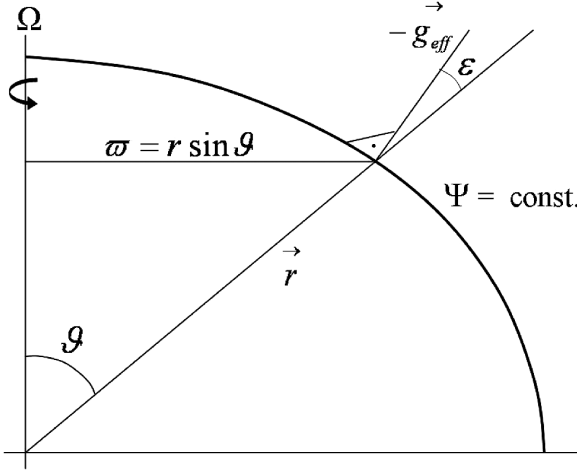


Fig. 2.1 Some geometrical parameters in a rotating star. The angle ε is the angle between the vector radius and the normal $-\mathbf{g}_{\text{eff}}$ to an equipotential

The components of \mathbf{g} are $(-g, 0, 0)$ and $g = \frac{\partial \Phi}{\partial r}$ (cf. 1.35). If Ω is constant or has a cylindrical symmetry, the centrifugal acceleration can also be derived from a potential, say V . One has

$$-\nabla V = \Omega^2 \boldsymbol{\varpi} \quad \text{and thus} \quad V = -\frac{1}{2} \Omega^2 \boldsymbol{\varpi}^2. \quad (2.3)$$

The total potential Ψ is

$$\Psi = \Phi + V, \quad (2.4)$$

and with (1.44) one has

$$\nabla^2 \Psi = \nabla^2 \Phi + \nabla^2 V \quad \text{with} \quad \nabla^2 \Phi = 4\pi G \varrho. \quad (2.5)$$

In cylindrical coordinates, one can write

$$(\nabla^2 V)_{\boldsymbol{\varpi}} = \frac{1}{\boldsymbol{\varpi}} \frac{\partial}{\partial \boldsymbol{\varpi}} (-\boldsymbol{\varpi}^2 \Omega^2) = -2\Omega^2 \quad (2.6)$$

and thus the Poisson equation with rotation becomes

$$\nabla^2 \Psi = 4\pi G \varrho - 2\Omega^2. \quad (2.7)$$

Barotropic star: the equation of hydrostatic equilibrium becomes

$$\frac{1}{\varrho} \nabla P = -\nabla \Psi = \mathbf{g}_{\text{eff}}. \quad (2.8)$$

The effective gravity \mathbf{g}_{eff} results from both gravitation and centrifugal acceleration. Care must be given on how Φ and Ψ are defined, since one often finds expressions with a different sign. The above expression implies that the pressure is constant on an equipotential, i.e., one has $P = P(\Psi)$. Thus, the equipotentials and isobars coincide in this case and the star is said to be *barotropic*, otherwise it is said to be *baroclinic* (Sect. 2.2). With $\nabla P = (dP/d\Psi) \nabla \Psi$, (2.8) becomes $(1/\varrho) dP/d\Psi = -1$. Thus, the density is also a function $\varrho = \varrho(\Psi)$ of Ψ only. Through the equation of state $P = P(\varrho, T)$, one also has $T = T(\Psi)$. The quantities ϱ , P , T are constant on the equipotentials $\Psi = \text{const.}$ The same conclusions are valid for Ω constant on cylindrical surfaces around the rotation axis.

2.1.3 Stellar Surface and Gravity

The stellar surface is an equipotential $\Psi = \text{const.}$, otherwise there would be “mountains” on the star and matter flowing from higher to lower levels. The total potential at a level r and at colatitude ϑ ($\vartheta = 0$ at the pole) in a star of constant angular velocity Ω can be written as

$$\Psi(r, \vartheta) = -\frac{GM_r}{r} - \frac{1}{2} \Omega^2 r^2 \sin^2 \vartheta. \quad (2.9)$$

One assumes in the Roche model that the gravitational potential $\Phi = -GM_r/r$ of the mass M_r inside radius r is not distorted by rotation. The inner layers are considered as spherical, which gives the same external potential as if the whole mass is concentrated at the center.

Let us consider a star of total mass M and call $R(\vartheta)$ the stellar radius at colatitude ϑ . Since the centrifugal force is zero at the pole, the potential at the stellar pole is just GM/R_p , where R_p is the polar radius. This fixes the constant value of the equipotential at the stellar surface, which is given by

$$\frac{GM}{R} + \frac{1}{2} \Omega^2 R^2 \sin^2 \vartheta = \frac{GM}{R_p}. \quad (2.10)$$

A more tractable form is given below (2.18). The shape of a Roche model is illustrated in Fig. 2.2 for different rotation velocities (the radii for non-rotating stars of different masses and metallicities Z are given in Fig. 25.7). Figure 2.3 illustrates the variation of the ratio of the equatorial radius to the polar radius for the Roche model as a function of the parameter $\omega = \Omega/\Omega_{\text{crit}}$. We see that up to $\omega = 0.7$, the increase of the equatorial radius is inferior to 10%. The increase of the equatorial radius essentially occurs in the high rotation domain.

The effective gravity resulting from the gravitational potential and from the centrifugal force is given by (2.8). If \mathbf{e}_r and \mathbf{e}_ϑ are the unity vectors in the radial and latitudinal directions, the effective gravity vector at the stellar surface is

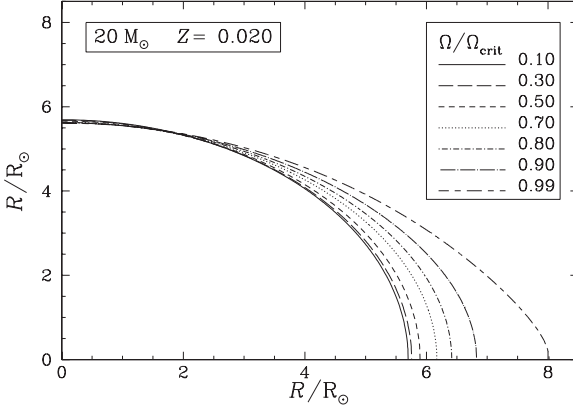


Fig. 2.2 The shape $R(\vartheta)$ of a rotating star in one quadrant. A $20 M_{\odot}$ star with $Z = 0.02$ on the ZAMS is considered with various ratios $\omega = \Omega/\Omega_{\text{crit}}$ of the angular velocity to the critical value at the surface. One barely notices the small decrease of the polar radii for higher rotation velocities (cf. Fig. 2.7). Courtesy of S. Ekström

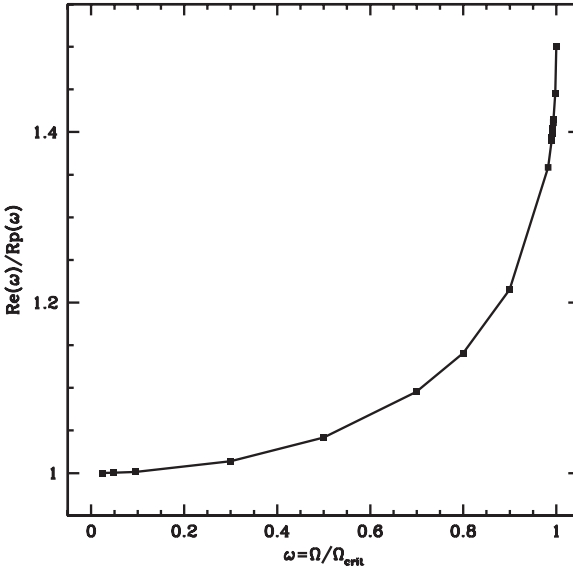


Fig. 2.3 The variation of the ratio R_e/R_p of the equatorial to the polar radius as a function of the rotation parameter ω in the Roche model

$$\mathbf{g}_{\text{eff}} = \left[-\frac{GM}{R^2(\vartheta)} + \Omega^2 R(\vartheta) \sin^2 \vartheta \right] \mathbf{e}_r + [\Omega^2 R(\vartheta) \sin \vartheta \cos \vartheta] \mathbf{e}_{\vartheta} . \quad (2.11)$$

The gravity vector is not parallel to the vector radius as shown in Fig. 2.1. The modulus $g_{\text{eff}} = |\mathbf{g}_{\text{eff}}|$ of the effective gravity is

$$g_{\text{eff}} = \left[\left(-\frac{GM}{R^2(\vartheta)} + \Omega^2 R(\vartheta) \sin^2 \vartheta \right)^2 + \Omega^4 R^2(\vartheta) \sin^2 \vartheta \cos^2 \vartheta \right]^{\frac{1}{2}}, \quad (2.12)$$

which can also be written as in (2.20).

2.1.4 Critical Velocities

The critical velocity, also called break-up velocity, is reached when the modulus of the centrifugal force becomes equal to the modulus of the gravitational attraction at the equator. The maximum angular velocity Ω_{crit} , which makes $g_{\text{eff}} = 0$ at the equator ($\vartheta = \pi/2$) is thus from (2.12)

$$\Omega_{\text{crit}}^2 = \frac{GM}{R_{\text{e,crit}}^3}, \quad (2.13)$$

where $R_{\text{e,crit}}$ is the equatorial radius at break-up. If one introduces this value of Ω_{crit} in the equation of the surface (2.10) at break-up, one gets for the ratio of the equatorial to the polar radius at critical velocity,

$$\frac{R_{\text{e,crit}}}{R_{\text{p,crit}}} = \frac{3}{2}. \quad (2.14)$$

At break-up, the equatorial radius is equal to 1.5 times the polar radius. The equatorial break-up velocity is thus

$$v_{\text{crit},1}^2 = \Omega_{\text{crit}}^2 R_{\text{e,crit}}^2 = \frac{GM}{R_{\text{e,crit}}} = \frac{2GM}{3R_{\text{p,crit}}}. \quad (2.15)$$

This expression is the one quite generally used; however, formally it applies to solid body rotation. The index “1” indicates the classical critical velocity, to distinguish it from a second value $v_{\text{crit},2}$ which applies to high mass stars with a high Eddington factor (see Sect. 4.4.2). If we now introduce a non-dimensional rotation parameter ω , defined as the ratio of the angular velocity to the angular velocity at break-up,

$$\omega = \frac{\Omega}{\Omega_{\text{crit}}} \quad \text{which gives} \quad \omega^2 = \frac{\Omega^2 R_{\text{e,crit}}^3}{GM}. \quad (2.16)$$

One can also write

$$\Omega^2 = \frac{8}{27} \frac{GM \omega^2}{R_{\text{p,crit}}^3}, \quad (2.17)$$

and the equation of the surface (2.10) becomes with $x = R/R_{\text{p,crit}}$

$$\frac{1}{x} + \frac{4}{27} \omega^2 x^2 \sin^2 \vartheta = \frac{R_{\text{p,crit}}}{R_{\text{p}}(\omega)}. \quad (2.18)$$

If the polar radius does not change with ω (but see Fig. 2.7), the second member is equal to 1. Equation (2.18) is an algebraic equation of the third degree. Our experience suggests it is better solved by the Newton method rather than by the Cardan solutions of a third degree polynomial, because the Cardan solutions may diverge at the poles. Also depending on the value of $R_{p,\text{crit}}/R_p(\omega)$, for ω close to 1 the discriminant of the polynomial equation may change its sign implying another form for the solution. The comparison with the interferometric observations of stellar oblateness and gravity darkening is given in Sect. 4.2.3.

Figure 2.4 shows the critical velocities $v_{\text{crit},1}$ for stars of various masses and metallicities. The critical velocities grow with stellar masses, because the stellar radii increase only slowly with stellar masses. The critical velocities are very large for low metallicity stars, since their radii are much smaller as a result of their lower opacities. Comparison between observed and theoretical values of velocities is given in Table 4.1. The distribution of rotational velocities for about 500 B-type stars is shown in Fig. 27.1.

Figure 2.5 shows the ratio $v/v_{\text{crit},1}$ of the equatorial velocity to the critical equatorial velocity as a function of the parameter $\omega = \Omega/\Omega_{\text{crit}}$ in the Roche model. For low rotation ($\omega < 0.5$), a linear approximation of v in terms of ω is valid

$$v^2 = \frac{8}{27} \frac{GM\omega^2}{R_{p,\text{crit}}^3} R_e^2 \approx \frac{8}{27} \frac{GM\omega^2}{R_{p,\text{crit}}} = \frac{4}{9} \omega^2 v_{\text{crit},1}^2, \quad (2.19)$$

as illustrated in Fig. 2.5. The relation of $(v/v_{\text{crit},1})$ vs. ω would be independent of stellar mass M and metallicity Z if the polar radius would not vary with rotation. As R_p is a function of ω which slightly depends on M and Z (cf. Fig. 2.7), this also introduces some slight dependence on mass and metallicity, not accounted for in the relation illustrated by Fig. 2.5.

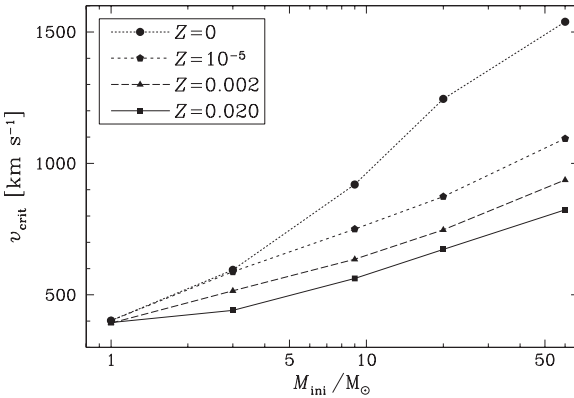


Fig. 2.4 The critical velocities $v_{\text{crit},1}$ as a function of stellar masses for different metallicities Z for stars on the ZAMS. The effect of the changes of the polar radius with rotation is accounted for. From S. Ekström et al. [176]

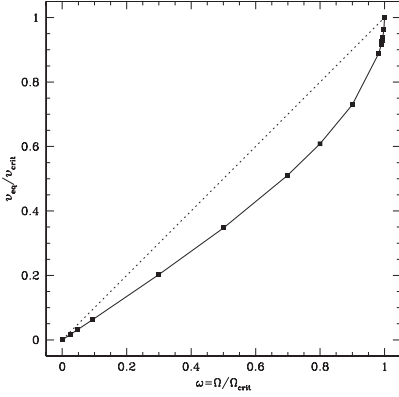


Fig. 2.5 The variation of the ratio $v/v_{\text{crit},1}$ of the equatorial velocity to the critical velocity as a function of the rotation parameter ω in the Roche model. The polar radius is assumed not to change with the stellar mass here. The *dotted line* connects the origin to the maximum value

The variations of the equatorial velocities v as a function of ω are illustrated for stars of different masses in Fig. 2.6. As the stellar radii change with M and Z , the relations of the velocities v with respect to ω are evidently different for the different masses and metallicities (in addition account is also given to the small effect of the change of the polar radius for the different M and Z , as mentioned above). The critical velocities for the most massive stars, where radiation pressure effects are large, are discussed in Sect. 4.4.

In terms of the parameters x and ω , the surface gravity at a colatitude ϑ on a rotating star can be expressed as

$$g_{\text{eff}} = \frac{GM}{R_{\text{p,crit}}^2} \left[\left(-\frac{1}{x^2} + \frac{8}{27} \omega^2 x \sin^2 \vartheta \right)^2 + \left(\frac{8}{27} \omega^2 x \sin \vartheta \cos \vartheta \right)^2 \right]^{\frac{1}{2}}, \quad (2.20)$$

where $GM/R_{\text{p,crit}}^2$ is the gravity at the pole at break-up. This is the maximum value and the term in square bracket is always smaller than 1.0.

Angle between \mathbf{g}_{eff} and \mathbf{r} : On the surface of a rotating star, the normal to the surface does not coincide with the direction of the vector radius (it coincides only at the pole and equator). There is an angle ε , generally small, between the directions of \mathbf{r} and of $-\mathbf{g}_{\text{eff}}$ (see Fig. 2.1)

$$\cos \varepsilon = - \frac{\mathbf{g}_{\text{eff}} \cdot \mathbf{r}}{|\mathbf{g}_{\text{eff}}| \cdot |\mathbf{r}|}. \quad (2.21)$$

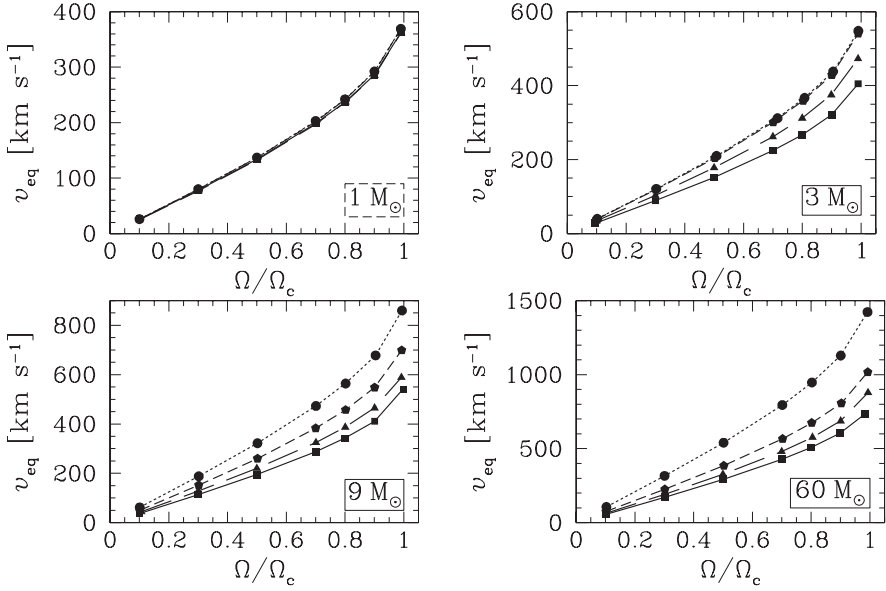


Fig. 2.6 Variations of the surface velocity v at the equator as a function of the rotation parameter $\omega = \Omega/\Omega_{\text{crit}}$ for stars of different masses and metallicities Z with the same coding as in Fig. 2.4. From S. Ekström et al. [176]

By using (2.11), one gets for the angle ε in terms of x and ω ,

$$\cos \varepsilon = \frac{\frac{1}{x^2} - \frac{8}{27} \omega^2 x \sin^2 \vartheta}{\left[\left(-\frac{1}{x^2} + \frac{8}{27} \omega^2 x \sin^2 \vartheta \right)^2 + \left(\frac{8}{27} \omega^2 x \sin \vartheta \cos \vartheta \right)^2 \right]^{\frac{1}{2}}}. \quad (2.22)$$

The angle ε intervenes in the expression of the surface element $d\sigma$ on an equipotential of a rotating star

$$d\sigma = \frac{r^2 \sin \vartheta d\varphi d\vartheta}{\cos \varepsilon}, \quad (2.23)$$

where φ is the longitude such that $\Omega = d\varphi/dt$. This means that the element of arc in ϑ along the real surface is slightly longer than the element of spherical arc (Fig. 2.1). The above expression is used in the calculation of the stellar surface and of the emergent flux from a rotating star.

2.1.5 Polar Radius as a Function of Rotation

In first approximation, one may consider that the polar radii are independent of rotation and use values such as given by Fig. 25.7. In reality the polar radii $R_p(\omega)$ have

a slight dependence on ω , which results from the small changes of internal structure brought about by centrifugal force. The rate of change is given by the models of internal structure with rotation. While the equatorial radius strongly inflates, the polar radius decreases by a few percent in general (Fig. 2.7), mostly as a result of a slight decrease of the internal T due to the lower effective gravity. Below $40 M_\odot$, the decrease of $R_p(\omega)$ at the critical velocity amounts to less than 2% [408]. Near $1 M_\odot$, the decrease of $R_p(\omega)$ with rotation is larger.

Surprisingly, at $60 M_\odot$ there is an increase of the polar radius with growing rotation (Fig. 2.7). This results from the fact that the radiation pressure is relatively important. As the temperature in the polar regions is much higher than at the equator as a result of von Zeipel's theorem (Sect. 4.2.2), the relative increase of the radiation pressure in the outer layers is much higher with a consequent inflation of the polar radius.

One may rather well represent the change of the polar radius as a function of ω by a form

$$R_p(\omega) = R_p(0) (1 - a \omega^2), \quad (2.24)$$

where a is a constant for models of a given mass [181]. Figure 2.8 provides information on the changes of polar radii at other Z values. It shows the changes of the polar radius at $\omega = 0.90$ for stars of different masses and metallicities. One again notices the general slight decrease of the polar radius at high rotation for most stellar masses, while the most massive stars in particular at the higher metallicities experience an increase.

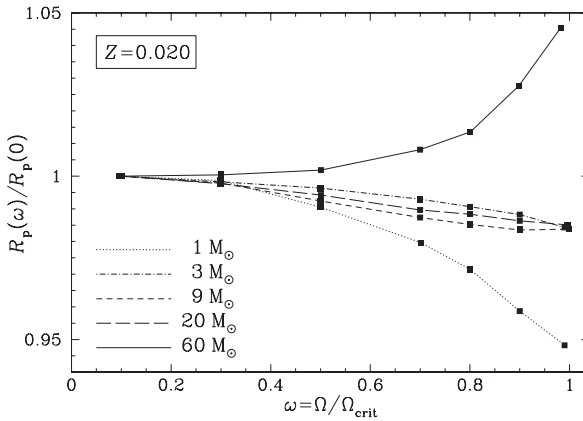


Fig. 2.7 Variations of the polar radius as a function of the rotation parameter ω normalized to the value without rotation for stars of different initial masses at $Z = 0.02$. From S. Ekström et al. [176]

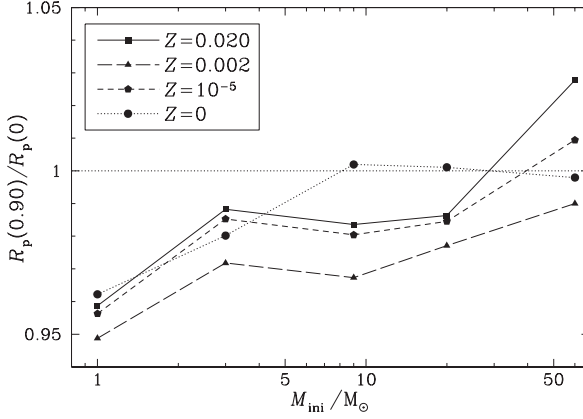


Fig. 2.8 Variations of the ratio of the polar radius at $\omega = 0.90$ to the value at zero rotation as a function of initial masses for different Z . Courtesy from S. Ekström

2.2 Equations of Stellar Structure for Shellular Rotation

Let us consider the interesting case of shellular rotation, where Ω is constant on isobars (i.e., surface of constant pressure), but varies according to the radial coordinate of the isobars. Rotation is shellular because differential rotation in radiative regions produces anisotropic turbulence [632], much stronger in the horizontal direction than in the vertical one due to stable stratification (Sect. 12.1). Since one has the relation $\nabla P = \mathbf{g}_{\text{eff}}$, the words “constant in the horizontal direction” mean constant on isobars, i.e., $\Omega = \Omega(P)$. One writes at a given point (r, ϑ) in spherical coordinates the angular velocity Ω

$$\Omega(r, \vartheta) = \overline{\Omega}(r) + \hat{\Omega}(r, \vartheta), \quad (2.25)$$

with $\hat{\Omega} \ll \overline{\Omega}$ (the average $\overline{\Omega}$ on an isobar with radius r is taken according to (10.105) so as to satisfy the equation for the conservation of angular momentum [632]). The quantity $\hat{\Omega}(r, \vartheta)$ can be developed in terms of the Legendre polynomials. The account of terms higher than the second order allows one to consider higher rotation velocities [386]. To the second order, one writes

$$\hat{\Omega}(r, \vartheta) = \Omega_2(r) P_2(\cos \vartheta). \quad (2.26)$$

This writing is sufficient for the approximation developed here. However, for the developments of $\Omega(r, \vartheta)$ used for the transport of angular momentum, one should rather write for consistency $\hat{\Omega}(r, \vartheta) = \Omega_2(r) [P_2(\cos \vartheta) + (1/5)]$. This is demonstrated in Appendix B.6.1, see also [386]. For the present purpose, we do not need to specify the development of $\hat{\Omega}(r, \vartheta)$. The different variables P , T , ϱ , etc. can be developed in Legendre polynomials (e.g., Sect. 11.1.1).

Let us emphasize that the isobars are not spherical surfaces. There is an angle ε (see Fig. 2.1) between the radial direction and the direction of gravity or between a spherical shell and an equipotential. As an example, in the Roche model at break-up rotation at a colatitude $\vartheta = 45^\circ$ this angle is 13° . For lower rotation, it rapidly decreases, behaving like Ω^2 . Thus, if one writes the shellular rotation as $\Omega \approx \Omega(r)$, one should not consider the cases of extreme rotation velocities.

2.2.1 Properties of the Isobars

In the case of shellular rotation, the centrifugal force cannot be derived from a potential and thus (2.3) does not apply. Let us consider the surface of constant Ψ (2.9),

$$\Psi = \Phi - \frac{1}{2}\Omega^2 r^2 \sin^2 \vartheta = \text{const.} \quad (2.27)$$

As in Sect. 1.2.1, the gravitational potential is defined by $\partial\Phi/\partial r = GM_r/r^2$ and $\Phi = -GM_r/r$ in the Roche approximation. The components of the gradient of Ψ are in polar coordinates (r, ϑ)

$$\frac{\partial\Psi}{\partial r} = \frac{\partial\Phi}{\partial r} - \Omega^2 r \sin^2 \vartheta - r^2 \sin^2 \vartheta \Omega \frac{\partial\Omega}{\partial r}, \quad (2.28)$$

$$\frac{1}{r} \frac{\partial\Psi}{\partial \vartheta} = \frac{1}{r} \frac{\partial\Phi}{\partial \vartheta} - \Omega^2 r \sin \vartheta \cos \vartheta - r^2 \sin^2 \vartheta \Omega \frac{1}{r} \frac{\partial\Omega}{\partial \vartheta}, \quad (2.29)$$

The first two components of the gravity $\mathbf{g}_{\text{eff}} = (-g_{\text{eff},r}, g_{\text{eff},\vartheta}, 0)$ are according to (2.11) in the Roche model,

$$\begin{aligned} g_{\text{eff},r} &= \frac{\partial\Phi}{\partial r} - \Omega^2 r \sin^2 \vartheta \quad \text{and} \\ g_{\text{eff},\vartheta} &= \Omega^2 r \sin \vartheta \cos \vartheta. \end{aligned} \quad (2.30)$$

Thus, by comparing these terms and the derivatives of Ψ , one can write

$$\mathbf{g}_{\text{eff}} = -\nabla\Psi - r^2 \sin^2 \vartheta \Omega \nabla\Omega. \quad (2.31)$$

The equation of hydrostatic equilibrium $\nabla P = \varrho \mathbf{g}_{\text{eff}}$ is thus

$$\nabla P = -\varrho (\nabla\Psi + r^2 \sin^2 \vartheta \Omega \nabla\Omega). \quad (2.32)$$

Since Ω is constant on isobars, the vector $\nabla\Omega$ is parallel to ∇P . The hydrostatic equation (2.32) implies the parallelism of ∇P and $\nabla\Psi$. Thus, in this non-conservative case the surfaces defined by $\Psi = \text{const.}$ (2.27) are isobaric surfaces [408], but they are not equipotential and the star is said to be *baroclinic*. In the case of solid body rotation, isobars and equipotentials coincide and the star is *barotropic*.

In literature, Ψ and Φ are often defined with different signs, care has to be given because this may lead to different expressions.

Thus, for shellular rotation one may choose to write the equations of the stellar structure on the isobars and use, with little changes, a method devised for the conservative case [283], with the advantage to keep the equations for stellar structure one-dimensional. The main change concerns the expression of the average density between isobars, as given below (cf. 2.47). Some further properties of baroclinic stars are studied in Sect. 10.5.3.

2.2.2 Hydrostatic Equilibrium

It is useful to write the equations of hydrostatic equilibrium and mass conservation in a form similar to that of the non-rotating case [283] in order to minimize the modifications necessary for calculating rotating stars with shellular rotation. One associates a radius r_P to an isobar, it is defined by

$$V_P \equiv \frac{4\pi}{3} r_P^3, \quad (2.33)$$

where V_P is the volume inside the isobar. For any quantity q , which is not constant over an isobaric surface, a mean value is defined by

$$\langle q \rangle \equiv \frac{1}{S_P} \oint_{\Psi=\text{const}} q d\sigma, \quad (2.34)$$

where S_P is the total surface of the isobar and $d\sigma$ is an element of this surface defined by (2.23).

The effective gravity can no longer be defined as a gradient $\mathbf{g}_{\text{eff}} = -\nabla\Psi$, since Ψ is not a potential. One uses the fact that $\nabla\Omega$ is parallel to $\nabla\Psi$,

$$\nabla\Omega = -\alpha \nabla\Psi \quad \text{with} \quad \alpha = \left| \frac{d\Omega}{d\Psi} \right|. \quad (2.35)$$

Let us call dn the average distance between two neighboring isobaric surfaces, ($dn \cong dr_P$). From (2.31), we get for the modulus of $\mathbf{g}_{\text{eff}} = (-g_{\text{eff},r}, g_{\text{eff},\vartheta}, 0)$,

$$g_{\text{eff}} = (1 - r^2 \sin^2 \vartheta \Omega \alpha) \frac{d\Psi}{dn}. \quad (2.36)$$

The equation of hydrostatic equilibrium (2.32) becomes similarly

$$\frac{dP}{dn} = -\varrho (1 - r^2 \sin^2 \vartheta \Omega \alpha) \frac{d\Psi}{dn}, \quad (2.37)$$

which shows the constancy of $\varrho (1 - r^2 \sin^2 \vartheta \Omega \alpha)$ on isobars.

We want to use the mass M_P inside an isobar as the independent variable,

$$\begin{aligned} dM_P &= \int_{\Psi=\text{const}} \varrho \, dn \, d\sigma = d\Psi \int_{\Psi=\text{const}} \varrho \frac{dn}{d\Psi} d\sigma \\ &= d\Psi \int_{\Psi=\text{const}} \varrho \frac{(1 - r^2 \sin^2 \vartheta \, \Omega \, \alpha)}{g_{\text{eff}}} d\sigma . \end{aligned} \quad (2.38)$$

The last equality is obtained by using (2.36). Since $\varrho (1 - r^2 \sin^2 \vartheta \, \Omega \, \alpha)$ is constant on isobars, we can easily integrate this equation by using also the definition (2.34)

$$\frac{d\Psi}{dM_P} = \frac{1}{\varrho (1 - r^2 \sin^2 \vartheta \, \Omega \, \alpha) < g_{\text{eff}}^{-1} > S_P} . \quad (2.39)$$

With (2.37), this becomes simply

$$\frac{dP}{dM_P} = \frac{-1}{< g_{\text{eff}}^{-1} > S_P} . \quad (2.40)$$

We define a quantity

$$f_P = \frac{4 \pi r_P^4}{G M_P S_P} \frac{1}{< g_{\text{eff}}^{-1} >} , \quad (2.41)$$

which is equal to 1.0 for a non-rotating star. With this definition the equation of hydrostatic equilibrium in Lagrangian coordinates finally becomes [408]

$$\frac{dP}{dM_P} = - \frac{G M_P}{4 \pi r_P^4} f_P . \quad (2.42)$$

Apart from the factor f_P , this equation keeps the same form as in the non-rotating case (cf. 1.15).

2.2.3 Continuity Equation

Similarly, we want an equation equivalent to (1.15) for shellular rotation. According to (2.33), the volume of a shell between two isobars is

$$dV_P = 4 \pi r_P^2 dr_P , \quad (2.43)$$

which can also be written as

$$\begin{aligned} dV_P &= \int_{\Psi=\text{const}} dn \, d\sigma = d\Psi \int_{\Psi=\text{const}} \frac{dn}{d\Psi} d\sigma \\ &= d\Psi \int_{\Psi=\text{const}} \frac{(1 - r^2 \sin^2 \vartheta \, \Omega \, \alpha)}{g_{\text{eff}}} d\sigma , \end{aligned} \quad (2.44)$$

where we have used (2.36). By applying (2.34), we get

$$dV_P = d\Psi S_P \left[\langle g_{\text{eff}}^{-1} \rangle - \langle g_{\text{eff}}^{-1} r^2 \sin^2 \vartheta \rangle \Omega \alpha \right]. \quad (2.45)$$

This expression together with (2.43) and (2.39) leads to

$$\frac{dr_P}{dM_P} = \frac{1}{4\pi r_P^2 \bar{\varrho}}, \quad (2.46)$$

$$\text{with} \quad \bar{\varrho} = \frac{\varrho (1 - r^2 \sin^2 \vartheta \Omega \alpha) \langle g_{\text{eff}}^{-1} \rangle}{\langle g_{\text{eff}}^{-1} \rangle - \langle g_{\text{eff}}^{-1} r^2 \sin^2 \vartheta \rangle \Omega \alpha}. \quad (2.47)$$

The quantity $\bar{\varrho}$ is not equal to $\langle \varrho \rangle$. From the definition (2.34), $\langle \varrho \rangle$ is the average density on an isobar, while from (2.46) we see that formally $\bar{\varrho}$ is the average density in the element volume between two isobars. When the mass steps are very small the difference between $\langle \varrho \rangle$ and $\bar{\varrho}$ becomes negligible; however, it is preferable to strictly respect the above definitions.

The two Eqs. (2.42) and (2.46) are the basic equations for the hydrostatic equilibrium of stars with shellular rotation [408], replacing the corresponding Eq. (1.15) of the case without rotation.

2.2.4 Equation of the Surface for Shellular Rotation

In the case of shellular rotation, the isobars are defined by expression (2.27), which is identical to the expression of the equipotentials for solid body rotation. We may search the equation of the equipotential, in particular for the stellar surface. An equipotential is defined by the condition that a displacement $d\mathbf{s}$ on it neither requires nor produces energy,

$$\mathbf{g}_{\text{eff}} \cdot d\mathbf{s} = 0. \quad (2.48)$$

The effective gravity is given by (2.31) and the above product becomes

$$\frac{\partial \Psi}{\partial r} dr + \frac{1}{r} \frac{\partial \Psi}{\partial \vartheta} r d\vartheta + r^2 \sin^2 \vartheta \Omega \frac{\partial \Omega}{\partial r} dr + r^2 \sin^2 \vartheta \frac{\Omega}{r} \frac{\partial \Omega}{\partial \vartheta} r d\vartheta = 0. \quad (2.49)$$

For shellular rotation, this equation simplifies to

$$d\Psi + r^2 \sin^2 \vartheta \Omega \frac{d\Omega}{dr} dr = 0. \quad (2.50)$$

This is a more general form of the equation of equipotentials (cf. 2.9). If $\Omega = \text{const.}$ it simplifies to $\Psi = \text{const.}$ and gives (2.10) again. Expression (2.50) can be integrated to give the equation of the stellar surface,

$$-\frac{GM}{R(\vartheta)} - \frac{1}{2} \Omega^2 R^2(\vartheta) \sin^2 \vartheta + \sin^2 \vartheta \int_{R_p}^{R(\vartheta)} r^2(\vartheta) \Omega \frac{d\Omega}{dr} dr = \frac{GM}{R_p}. \quad (2.51)$$

This equation gives the shape $R(\vartheta)$ of the star as a function of $\Omega(r)$ in the external regions. If $d\Omega/dr < 0$ in the external layers, the above expression indicates that the real oblateness of the star is slightly larger than the one which would be obtained by using the Ω value effectively observed at the equator. In general, in the outer stellar layers the gradient $d\Omega/dr$ is nearly flat, thus the difference with respect to the usual Roche surface should be small. We have assumed that the gravitational potential of the inner layers is still the potential of a spherical object, which is satisfactory for evolution in the H-burning phase, but maybe not in advanced stages where central rotation may become very high. Interferometric observations are reported in Sect. 4.2.3.

The above developments allow us to construct equilibrium models of rotating stars in one dimension, which is most useful in view of the calculation of grids of evolutionary models of rotating stars. Ignoring the effects of rotation on the structure equations leads to incomplete models. We emphasize that in general the main effects of rotation on the evolution are those due to the internal mixing of the chemical elements, to the transport of angular momentum and to the enhancement of the mass loss in massive stars. These effects are studied in further chapters.

<http://www.springer.com/978-3-540-76948-4>

Physics, Formation and Evolution of Rotating Stars

Maeder, A.

2009, XXI, 832 p. 325 illus., 6 illus. in color., Hardcover

ISBN: 978-3-540-76948-4